Integration of Preferences in Hypervolume-Based Multiobjective Evolutionary Algorithms by Means of Desirability Functions

Tobias Wagner and Heike Trautmann

***Abstract*—In this paper, a concept for efficiently approximating the practically relevant regions of the Pareto front (PF) is introduced. Instead of the original objectives, desirability functions (DFs) of the objectives are optimized, which express the preferences of the decision maker. The original problem formulation and the optimization algorithm do not have to be modified. DFs map an objective to the domain [0, 1] and nonlinearly increase with better objective quality. By means of this mapping, values of different objectives and units become comparable. A biased distribution of the solutions in the PF approximation based on different scalings of the objectives is prevented. Thus, we propose the integration of DFs into the $\mathcal{S}$-metric selection evolutionary multiobjective algorithm. The transformation ensures the meaning of the hypervolumes internally computed. Furthermore, it is shown that the reference point for the hypervolume calculation can be set intuitively. The approach is analyzed using standard test problems. Moreover, a practical validation by means of the optimization of a turning process is performed.**

***Index Terms*—Desirability function, hypervolume indicator, preferences, SMS-EMOA.**

I. Introduction

MULTIOBJECTIVE optimization (MOO) focuses on the approximation of a set of optimal solutions for optimization problems having $k > 1$ objectives. Compared to the approximation of a single optimal solution, the approximation of a whole set inevitably demands a higher computational effort, making MOO often inapplicable for expensive real-world problems. In contrast, a single-objective formulation can often only insufficiently describe all problem features. The incorporation of the decision maker (DM)'s preferences into the multiobjective formulation can provide a compromise solution to this conflict by restricting the approximation to the region of the multiobjective space which is of practical interest. Only in this region, the optimal tradeoffs of the objectives are approximated, saving additional resources otherwise spent by the MOO algorithm. In particular in engineering, such regions are often motivated by engineer standards.

In recent years, the use of set quality indicators has become established to solve MOO problems [1]–[3]. Among other indicators, especially the hypervolume dominated by the set with respect to a fixed reference point has obtained popularity since it is compatible with the dominance relation and evaluates both properties desired in MOO, convergence toward better solutions, and a wide and well-distributed spread within the Pareto front (PF) approximation [4]. During the hypervolume calculation, k-dimensional hypervolumes over different objectives such as product quality and costs are computed. For an engineer or physicist, who is concerned about the units of values, this is rather confusing. Furthermore, a reference point is required that is dominated by all solutions to compare. In practical problems, where the domain of the objectives is often *a priori* unknown, the definition of an appropriate reference point is hard to accomplish.

Desirability functions (DFs) are a flexible yet mathematically simple description of preferences. Each objective is individually transformed into a desirability, i.e., a normalized value in the domain [0, 1]. The smaller the distance between the desirability and its maximum value of 1 the more satisfying the quality of the objective value. By means of the nonlinear shape of the well-known Harrington DF, which expresses an asymptotic behavior toward low and high desirabilities, infeasible objective values as well as complete satisfaction can be integrated in the DF specification [5]. Consequently, the tradeoffs between the objectives change for different objective levels. Thus, nonlinear interactions between the objectives can be expressed even if the definition of the DFs is done objective-wise.

By operating on the same objective scales, an unintentionally induced weighting of different objectives is prevented. As stated by Branke and Deb [6], different objective scales lead to biased distributions of the solutions on the PF, i.e., "... the user-defined scaling is actually a usually ignored form of user preference specification ...." Furthermore, the transformation allows the reasonable calculation of hypervolumes since all values are given in the same unit. The most common desirability index (DI), i.e, a scalarization of a desirability vector, is defined as the geometric mean [5], which is basically a product and relates to the hypervolume indicator.

Manuscript received September 16, 2009; revised January 6, 2010; accepted June 1, 2010. Date of current version October 1, 2010. This paper is based on investigations of the collaborative research centers, Sonderforschungsbereich/Transregional Collaborative Research Center 30 and SFB 823, which are kindly supported by the Deutsche Forschungsgemeinschaft (German Research Foundation).

T. Wagner is with the Institute of Machining Technology, Technische Universität Dortmund, 44227 Dortmund, Germany (e-mail: wagner@isf.de).

H. Trautmann is with the Department of Computational Statistics, Technische Universität Dortmund, 44221 Dortmund, Germany (e-mail: trautmann@statistik.uni-dortmund.de).

Color versions of one or more of the figures in this paper are available online at http://ieeexplore.ieee.org.

Digital Object Identifier 10.1109/TEVC.2010.2058119

TABLE I
SELECTED IMPORTANT APPROACHES FOR INCORPORATING USER PREFERENCES [9]

Topic	Information	Modification	Effect
Constraints [14]	Constraint	Feasible search space	Range
Preference relation [22]	Reference point	Dominance	Range
Reference point MOO [23]	Reference point	Crowding distance	Range
Light beam search-based MOO [24]	Reference direction thresholds	Crowding distance	Range
Imprecise value function [25]	Solution ranking	Dominance	Range
Guided EMOA [21]	Max./min. tradeoff	Objectives	Range
Weighted integration [26]	Weighting of objective space	Crowding distance	Distribution
Marginal expected utility [15]	Tradeoff probability distribution	Crowding distance	Distribution
Biased crowding [6]	Desired tradeoff	Crowding distance	Distribution

Consequently, in this paper, a hypervolume-based evolutionary multiobjective algorithm (EMOA) operating on objectives which are individually transformed by DFs is introduced and empirically validated. To accomplish this task, both test functions and a real-world production-engineering problem are considered. In Section II, the state-of-the-art in preference-articulation techniques within EMOAs is summarized, classified, and the new approach is integrated within this research. A short introduction to DFs is provided in Section III. Thereafter, the integration of DFs in the framework of the $\mathcal{S}$-metric selection-based EMOA (SMS-EMOA) [7], [8], which is one of the most famous hypervolume-based EMOA, is presented. In this context also enhancements to forestall numerical issues generated by the transformation are proposed. The approach is empirically validated in Section V. The experiments are designed to answer the following five main questions.

1) Does the approach allow the restriction to parts of the PF?
2) How is the distribution of solutions in the approximation set biased by the transformation?
3) How sensitive is the approach with respect to target regions on and far from the true PF?
4) Does the incorporation of preferences have an effect on the global search behavior of the algorithm?
5) Are the preferences on objectives of real-world problems adequately expressed in the resulting approximation set?

In Section VI, the paper is summarized and conclusions are drawn.

II. STATE-OF-THE-ART

In recent years, the computation of a subset of Pareto-optimal solutions that agrees with the preferences of the DM has become a very important and still ongoing research topic. The consideration of these preferences is always a key factor in MOO since an approximation set of practically relevant solutions within the desired objective ranges significantly supports the final decision making. Consequently, multiple overviews of existing approaches have already been given [9]–[11]. A review with respect to interactive methods has been provided by Jaszkiewicz and Branke [12]. Adra *et al.* [13] have focused on preference incorporation within many-objective problems. In the most recent survey, Branke [9] has categorized concepts based on the type of required preference information. These types are objective scaling, weighted performance measures, additional constraints, optimization with respect to a goal or reference point, and the utilization of tradeoff information. The approaches introduced in [6], [14], and [15] were presented as a selection of the most important concepts so far. Branke [9] has classified these approaches as shown in Table I. The information required from the DM is considered, as well as the kind of modification of the EMOA. Furthermore, the information is provided whether the preference articulation has an effect on the range or the distribution of the approximation set.

In Table II, we propose an alternative classification of the important articles so far. We classified them with respect to two criteria—requirement for an online interaction (rows) and locus of the preference articulation (column). For instance, Coello Coello [14] proposed the *a priori* integration of preferences by transforming them into constraints. Consequently, no online interaction is necessary, but the number of constraints increases, leading to a change of the optimization problem. Branke and Deb [6] introduced a biased crowding distance measure which results in a biased distribution of the final PF. This causes a modification of the selection process and, thus, a modification of the EMOA itself.

The approach proposed in this paper belongs to the category "Change of objectives/no interaction." The concepts in this category can be easily applied since the transformed objective functions can be optimized without performing modifications on the EMOA. In addition, the dimension of the problem or the number of constraints are not increased by changing the problem structure. Thus, we restrict the following summary of the state-of-the-art to approaches of this category.

Preliminary versions of the approach proposed in this paper have already been introduced [16], [17]. In these papers, DFs were integrated into NSGA-II [18], and extensions to noisy environments were proposed. The concept of DFs is now combined with $\mathcal{S}$-metric selection, and a procedure to overcome numerical difficulties related to the DF transformation is introduced. Up to now, only three papers have reported on approaches comparable to the one presented in this paper. Messac [19] introduced physical programming (PP), which can be seen as a very general concept for constructing desired ranges of the objective functions—similar to DFs. By means of a PP lexicon, desirability ranges are defined classifying the domain of the objective function in six classes from "unacceptable" to "highly desirable." Afterward, an aggregate preference function can be calculated based on individual preference values for the classes. Utyuzhnikov *et al.* [20] presented a

TABLE II
CLASSIFICATION OF EXISTING APPROACHES FOR INCORPORATING USER PREFERENCES INTO EMOA

Change of Interaction	Problem	Objectives	EMOA
Yes	[27], [28]	[29]	[22], [30]–[34]
No	[14]	[16], [17] [19]–[21]	[6], [15], [23]–[26] [35]–[41]

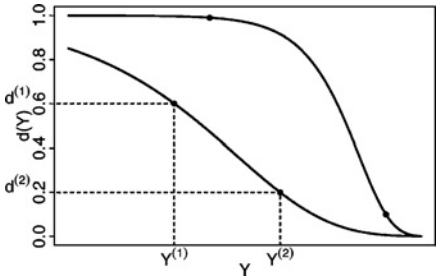

Fig. 1. Two realizations of Harrington's one-sided DF based on the specified 2-tuples depicted as black dots.

modified PP method, which generates PF approximations with an even distribution along a desired part of the original PF. Though obtaining similar results as the approach presented in this paper, the PP method is more complex and requires the specification of a much higher number of parameters. For the use of the guided dominance [21], maximally acceptable tradeoffs for each pair of objectives have to be specified. Thus, this approach performs rather a weighting of the objectives than an individual definition of preferred objective ranges, i.e., the objectives are treated as not equally important.

III. DESIRABILITY FUNCTIONS AND THE DESIRABILITY INDEX

The concept of desirability was introduced by Harrington [5] in the context of multiobjective industrial quality control. DFs map the values of the objectives to desirabilities, i.e., values on a unitless scale in the domain $[0, 1]$. The mapping is based on preference information regarding exemplary objective values. The preferences are specified under the assumption that the smaller the difference between the actual desirability and the maximum value of one, the better the quality of the solution in the corresponding objective. In general, any function $d : Y \rightarrow [0, 1]$ describing the desirability of different regions in the objective space can be defined as a DF [17], [42]. Harrington introduced two types of DFs. The first DF is suited for the maximization or minimization of the objectives (one-sided specification). Two DFs of this type are shown in Fig. 1. The second DF type was designed for target value problems (two-sided specification). Three two-sided DFs having different shapes are depicted in Fig. 2.

Harrington's one-sided DF realizes a special form of the Gompertz-curve [43] for an objective Y

$$d(Y) = \exp(-\exp(-(b_0 + b_1 Y))). \tag{1}$$

In order to find suitable values b_0 and b_1 for the definition of the DF, two 2-tuples of an objective value and a corresponding

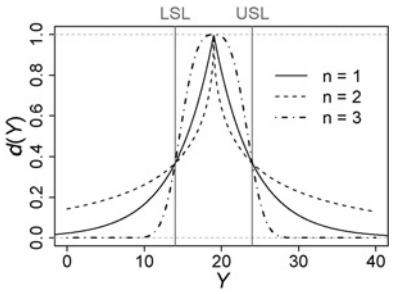

Fig. 2. Three realizations of Harrington's two-sided DF based on different values of the exponent n.

desirability are required, denoted by $(Y^{(1)}, d^{(1)})$ and $(Y^{(2)}, d^{(2)})$. These values are represented as black dots in Fig. 1. In industrial applications of this DF, $d^{(1)} \approx 0.99$ and $d^{(2)} \approx 0.01$ are usually fixed, and two thresholds which represent an absolutely satisfying and a marginally infeasible objective value are specified. More specific, the shape of the function is determined by the solutions

$$b_0 = -\log(-\log(d^{(1)})) - b_1 Y^{(1)},$$
$$b_1 = (-\log(-\log(d^{(2)})) + \log(-\log(d^{(1)})))/(Y^{(2)} - Y^{(1)})$$

to the two equations

$$d^{(i)} = \exp(-\exp(-(b_0 + b_1 Y^{(i)}))) \; i = 1, 2 \tag{2}$$

based on the 2-tuples $(Y^{(1)}, d^{(1)})$ and $(Y^{(2)}, d^{(2)})$ specified before.

Harrington's two-sided DF requires an upper (USL) and a lower specification limit (LSL) for an objective Y. These limits are mapped to a desirability of $1/e \approx 0.37$. The target value is assumed to be in the center of the specification limits. The desirability $d(Y)$ for other objective values is defined as follows:

$$d(Y) = \exp(-|Y'|^n) \qquad Y' = \frac{2Y - (USL + LSL)}{USL - LSL}.$$

The parameter $n > 0$ determines the shape of the function and can be adjusted to adequately describe the preferences of the DM (compare Fig. 2).

The DI combines the individual DFs into a single-objective preference index which can be used to assist the DM by ranking the solutions in the PF approximation. It is also defined in the interval $[0, 1]$ and has the intuitive interpretation that the better the quality of the compromise with respect to the preferences encoded in the DFs, the higher the DI. Thus, it represents a univariate and unitless measure for the compromise quality. The individual on the final front with the highest DI would be the first candidate to be chosen by the DM who specified the DFs. Furthermore, a more sophisticated reduction of multiobjective problem formulations into single-objective ones can be realized by directly optimizing the DI [5], [42].

For k objectives Y_j $(j = 1, \ldots, k)$ the DI most generally is defined as any scalarizing function $D : [0, 1]^k \rightarrow [0, 1]$ with $(d_1(Y_1), \ldots, d_k(Y_k)) \rightarrow D(Y_1, \ldots, Y_k)$. Harrington [5]

Require: $\vec{d}$: $(Y_1^{(1)}, d_1^{(1)})$ $(Y_1^{(2)}, d_1^{(2)})$ $\vdots$ $(Y_k^{(1)}, d_k^{(1)})$ $(Y_k^{(2)}, d_k^{(2)})$

{Definition of the DFs for each of the k objectives}

1: Random initialization and evaluation of the population
2: **repeat**
3: Reset DFs according to $\vec{d}$
4: Binary tournament selection of parent individuals
5: Simulated binary crossover (SBX) and polynomial mutation (PM) [46, pp. 106ff] of the parents and evaluation of the offspring
6: **for** $j = 1, \ldots, k$ **do**
7: $y_{med,j} = \text{median}(\vec{f_j})$ {Determine median value of objective f_j in the population}
8: **if** $d_j(y_{med,j}) < \varepsilon$ **then**
9: $Y_j^{(2)} = y_{med,j}$
10: $d_j^{(2)} = \varepsilon$ {Adjust to avoid numerical problems with respect to the machine accuracy ε}
11: **end if**
12: $\vec{f_j} = -d_j(\vec{f_j})$ {Transform objectives $\vec{f_j}$ in desirabilities using the adjusted DFs}
13: **end for**
14: Perform non-dominated sorting [47] to identify the m individuals in the last front $\mathcal{F}_{last}$
15: **for** $i = 1, \ldots, m$ **do**
16: $HV_{-i} = hypervolume(\mathcal{F}_{last} - \vec{f}^{(i)}, \mathbf{0})$ {Compute hypervolume of the last front without the i-th individual using the reference point $\mathbf{0}$}
17: **end for**
18: Reject individual $\vec{f}^{(i)}$ with highest HV_{-i}
19: **until** termination criterion is met

Fig. 3. Pseudocode of the DF-SMS-EMOA.

proposed the aggregation approach of computing the geometric mean of the DFs as follows:

$$D_{\text{GM}} := \left(\prod_{j=1}^{k} d_j(Y_j) \right)^{1/k} \qquad j = 1, \ldots, k. \tag{3}$$

The maximum value of one is only achieved if all DFs attain the maximum value. In contrast, a desirability of zero results in cases where at least one of the objectives is infeasible.

As an alternative to D_{GM}, the more conservative scalarization

$$D_{\text{MM}} := \min_{j=1,\ldots,k} d_j(Y_j) \qquad j = 1, \ldots, k \tag{4}$$

can be used [44]. This DI shares the good properties of the geometric mean D_{GM}, but puts a stronger focus on the objective with the worst desirability by maximizing the minimum of the individual DFs.

Both scalarization approaches, D_{GM} and D_{MM}, show the characteristic property of the DFs to allow for a nonlinear weighting of different objectives with regard to the current objective values of a given compromise solution. In the beginning of the optimization, the value of one objective may be outside the specification limits. Consequently, the DFs will lead to a focus on the optimization on this objective. As soon as all objectives are in their desired range, the weighting between the objectives will become uniform. Thus, even though the definition of the DFs is done objective-wise, nonlinear interactions between the objectives in the course of the optimization can be considered.

The weighted sum (WS)

$$D_{\text{WS}} := \sum_{j=1}^{k} w_j \cdot d_j(Y_j) \qquad j = 1, \ldots, k \tag{5}$$

is frequently used in practice in order to scalarize objective vectors. However, in combination with the DF transformation, the WS has several drawbacks. The property of being zero in case at least one DF equals zero is not met. Solutions in concave regions of the front cannot be obtained. The specification of different weights is necessary and the objectives are no longer treated as equally important, as soon as all objectives are in their desired ranges. Moreover, the property of D_{GM} to stress on compromises where all objectives are in a desired range is at least weakened.

IV. Combination of Desirability Functions and S-Metric Selection

In this section, the integration of DFs into the SMS-EMOA [8] (DF-SMS-EMOA) is presented. The SMS-EMOA is chosen as the combination of a hypervolume-based EMOA and the DFs show several synergistic benefits, such as a computation of volumes over the same units, an *a priori* known domain for the reference point definition, and the relation of the hypervolume to the geometric mean DI D_{GM} (3). Nevertheless, the procedure of the DF-SMS-EMOA proposed in Fig. 3 can be used with any EMOA by exchanging lines 1, 4–5, and 14–18 with the variation and selection mechanisms of the desired EMOA.

The DFs, *a priori*, are defined for each of the k objectives. Harrington's one-sided DF (2) has been chosen for the transformation $d(Y)$ since it can express a wide range of shapes while still being intuitive to parameterize. As mentioned in Section III, the shape of Harrington's one-sided DF can be described by just two 2-tuples $(Y^{(1)}, d^{(1)})$ and $(Y^{(2)}, d^{(2)})$. Thus, these tuples are required beforehand for each objective in order to specify the DFs.

The monotonicity of the one-sided Harrington DF sustains the dominance relations between the solutions defined by the original objectives. Different DFs, e.g., for target value problems, can be integrated straightforwardly, noting that the dominance relation between the individuals and the required parameters may be changed. Based on the DF transformation, all objectives can be compared on the same scale. No modifications on the selection mechanism, as well as on the generation and variation of individuals, have to be performed. Thus, the objective vectors are transformed into desirabilities using DFs (line 12) after the evaluation of the solutions, leading to the problem formulation as follows:

$$\min_{X \in \mathcal{X}} \quad -\vec{d}(Y) = -(d_1(f_1(X)), \ldots, d_k(f_k(X)))^T.$$

After the transformation of the objectives, the hypervolume-based selection is performed (lines 14–18). First, a nondominated sorting [46] is accomplished by iteratively removing

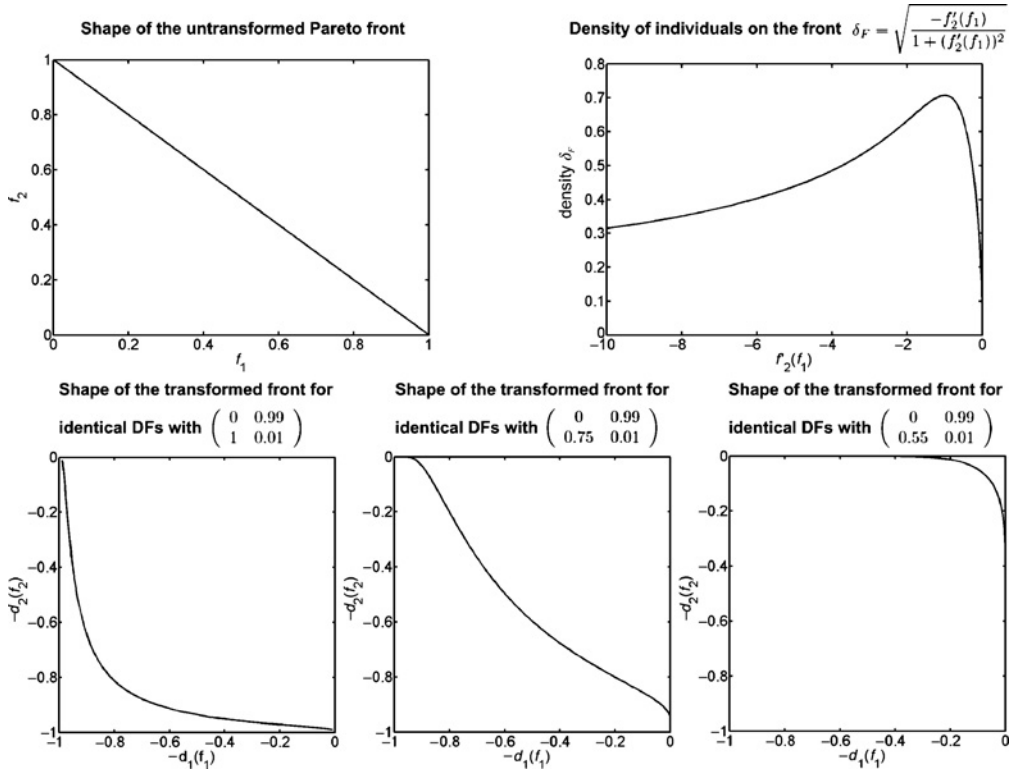

Fig. 4. Shape of the PF $f_2 = 1 - f_1$ (upper left plot) in desirability space for different parameterizations of the DFs. The hypervolume-optimal density δ_F of individuals on the front with respect to the derivative $f_2'(f_1)$ is plotted according to a formula derived by Auger *et al.* [47] (upper right plot).

the nondominated individuals (line 14). By these means, the population is clustered into fronts of individuals which do not dominate each other. For the last of these fronts, containing only individuals which do not dominate any other individual in the population, the hypervolume contribution [8] is computed for each individual (lines 15–17). This is accomplished by removing the individual from the front and computing the hypervolume of the remaining individuals. The individual with the lowest contribution, i.e., the highest hypervolume of the remaining individuals, is removed. This steady-state or $(\mu+1)$-strategy ensures a monotonic increase of the hypervolume dominated by the population.

For two and three objectives, the hypervolume computation is of the same complexity $O(\mu \log(\mu))$ as the nondominated sorting procedure. For more than three objectives, the runtime increases in $O(\mu \log(\mu) + \mu^{(d/2)})$ [48]. For practical problems, where an evaluation often requires expensive simulations, this is not crucial as long as the number of objectives d is moderate, e.g., $d \leq 6$. However, a different EMOA may be chosen for problems having a large number of objectives. As mentioned before, the integration of DFs is not necessarily coupled to the SMS-EMOA, even though their combination shows some synergistic benefits, as we will describe in the following.

The effect of the DF transformation is shown in Fig. 4 by means of different shapes of the PF in desirability space. The plots are analytically computed by transforming the original PF with different DFs. With regard to the proposed DF-SMS-EMOA, the DFs are depicted as $-d_j(f_j)$, which results in minimization problems in both spaces. For the sake of simplicity, a linear biobjective original PF $f_2 = 1 - f_1$ has been chosen. It is known that the hypervolume-optimal density of individuals on this PF is uniform [8], [47]. Moreover, the DFs are the same for both objectives, leading to a focus on the center of the PF. However, a focus on different parts of the PF will lead to the same results since the PF is linear over the whole domain. An experimental analysis of different focus regions for nonlinear PFs is performed in the next section. The unimodal shape of Harrington's DFs only allows the focus on a single region of the PF. For a focus on different regions, multimodal functions have to be defined as DF, e.g., periodic trigonometric functions, such as the sine or cosine function, but this is beyond the scope of this paper.

In cases where the specified region covers the whole PF, the shape of the front changes from linear in the objective space to convex in the desirability space (bottom left plot in Fig. 4). Based on the findings of Auger *et al.* [47] for biobjective PFs, the density of individuals in a hypervolume-optimal approximation is only based on the first derivative $f_2'(f_1)$, where the maximum density is obtained for derivatives close to one (upper right plot of Fig. 4). Thus, the transformation causes a strong change of the focus toward the knee of the PF. Consequently, the approximation will be biased toward solutions having desirable values in both objectives, which is closely related to the desirability indices D_{GM} and D_{MM} (compare Section III). The characteristic property of the DFs to allow for a nonlinear weighting of different objectives with regard to the current objective values of a given compromise solution can be integrated into the EMOA. The same holds for the nonlinear interaction between the objectives in the course of the optimization described at the end of Section III.

When the low desirability limits $(Y^{(2)}, d^{(2)})$ are moved closer to the PF, the shape of the PF in desirability space changes from convex over concave–convex to concave (bottom of Fig. 4). However, two properties of the transformed PF remain over all three DFs considered in Fig. 4. First, derivatives close to one are mainly located in the area of compromise solutions, and, second, the derivatives at the extremes of the PF are close to zero or $-\infty$, leading to a very low density of solutions on these extremes (compare upper right plot of Fig. 4). Moreover, in a hypervolume-optimal approximation set of finite size, the extreme points will not be covered for any finite reference point in cases where the derivatives at the extremes of the PF are zero or $-\infty$ [47]. Since the extreme points have zero desirabilities in at least one objective, this effect is strongly intended. Furthermore, the optimal position of the outer individuals will move toward compromise solutions for closer reference points [47]. As the DF-transformed objectives are in the domain $[-1, 0]$ with minus one being the best and zero being the worst (line 11), the reference point $\boldsymbol{R} = \boldsymbol{0}$ can be recommended since it is the closest reference point which is dominated by any possible desirability vector.

The bottom right plot of Fig. 4 shows that a narrow specification of the DFs leads to very low desirabilities, even for a huge part of the PF. Consequently, in cases where the region of the PF is small with respect to the complete objective domain, desirabilities below the machine accuracy[1] are likely to appear, leading to incomparable objective values in the transformed domain. Thus, after the evaluation of the updated population, we propose a check whether the desirability of the median value of each objective falls below this threshold (lines 7–8). If this situation occurs, the corresponding DF is adjusted to guarantee for a sufficient selection pressure (lines 9–10). Since the DFs are reset at each iteration (line 3), the actually defined DFs are used when the population approaches the target region. By these means, no manual adaption in the course of the optimization is necessary while numerical problems which may arise by the DF transformation are avoided.

V. Experiments

In this section, the main research questions of Section I and the theoretically motivated assumptions about the behavior of the DF-SMS-EMOA of Section IV are empirically tested. The parameter settings of the DF-SMS-EMOA are listed in Table III. The questions 1)–3) are analyzed by applying the DF-SMS-EMOA on the shifted and rotated versions of the 30-dimensional, biobjective test functions ZDT1, ZDT2, and ZDT3 [49] in Section V-A. Then in Section V-B, it is analyzed on the 10-dimensional, rotated variant of the multimodal biobjective test function ZDT4 whether the restriction on parts of the PF has an effect on the global search quality of the EMOA, as stated in question 4). In the last experiment in Section V-C, DF-SMS-EMOA is validated by means of a practical problem from machining. More specific, the parameters of a turning process have to be optimized for given specification limits of the surface quality, the tool wear, and the production time. By means of this experiment, question 5) can be evaluated.

[1]We use the accuracy $\varepsilon \approx 1.1 \times 10^{-16}$ according to the MATLAB constant eps.

TABLE III
Parameter Setting of SMS-EMOA (MATLAB-Implementation)

				SBX			PM	
Problem	*dim*	♯ FE	μ	p_c	η_c	p_{swap}	p_m	η_m
ZDT1-3	30	10 000					$\frac{1}{30}$	
ZDT4	10	20 000	100	0.9	15	0.5	0.1	20
Turning	3	20 000					$\frac{1}{3}$	

In the experiments on ZDT1-ZDT3 and on the turning problem, results of representative experiments based on a small set of runs are described. On ZDT4, the number of FE and repetitions are increased to 20 000 and 50, respectively. This is done since the experiments served as a proof of principle for the new approach in the former case. In contrast, the ZDT4 experiment has a benchmark character where differences between variants of the SMS-EMOA with and without preferences are to be detected.

A. Proof of Principle

The test functions ZDT1, ZDT2, and ZDT3 are chosen in order to evaluate the integration of preferences in the DF-SMS-EMOA for convex and concave, as well as connected and disconnected PFs. ZDT1 and ZDT2 have connected convex and concave PFs, respectively. The PF of ZDT3 is disconnected and has concave and convex parts. Different instantiations of the DFs were realized in order to focus on different parts of the PF. In all figures, the region of desirabilities $d \in [0.001, 0.999]$ is emphasized in gray color in order to visualize the specified preference region, e.g., the objective range with the highest desirability gradients. This region is denoted as target region in the following. Recall that better objective values are still improving the desirability since one-sided preferences are used. The DF-SMS-EMOA was biased to the center, the upper left, and the lower right part of the connected PFs (Figs. 5 and 7). For the disconnected PF, restrictions to single PF parts and combinations of PF parts were specified (Fig. 8). The specified target regions are not symmetrical with respect to the objectives for two reasons. First, the PFs of ZDT1, ZDT2, and ZDT3 are not symmetrical. Second, different spreads of the target regions show the robustness of the approach with regard to the target specification.

These experiments were conducted to analyze whether the bias toward parts of the PF can be reflected in the PF approximations of the DF-SMS-EMOA.

Representative PF approximations of the DF-SMS-EMOA for different DF parameterizations are shown in Figs. 5, 7, and 8. The DF-SMS-EMOA strongly biases the approximation set toward the desired part of the PF. Only one or two solutions are outside the highlighted area. In Fig. 6, the PF approximations of the DF-SMS-EMOA on ZDT1 are shown in desirability space. The shapes of the fronts in desirability space are in line with the ones of Section V-A and are mainly dependent on the relative position of the target region and the section of the PF considered in this region. Moreover, the density of solutions agrees with theory (compare Fig. 4), showing

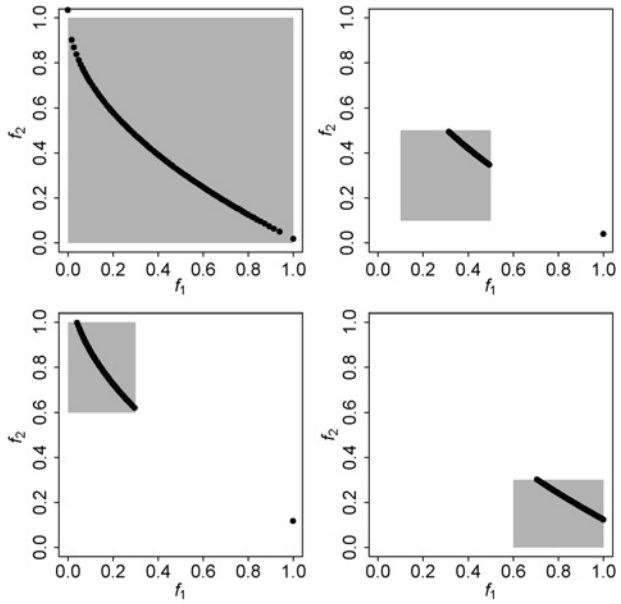

Fig. 5. Representative PF approximations of the DF-SMS-EMOA on ZDT1. The different target regions are highlighted by gray boxes, which indicate the area of the objective space mapped to desirabilities $d_i \in [0.001, 0.999]$, $i = 1, 2$.

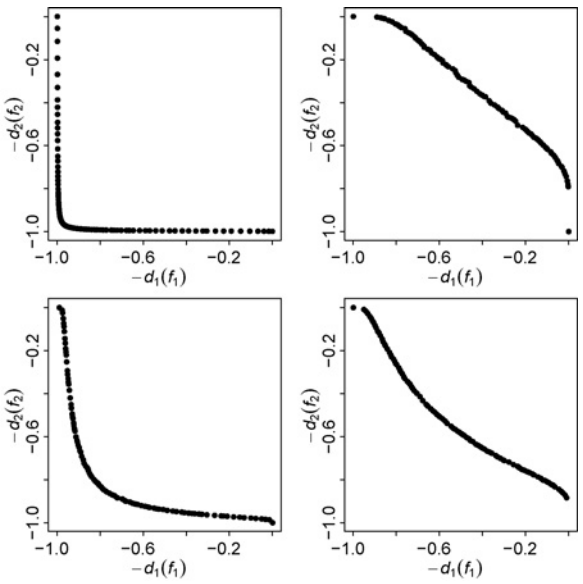

Fig. 6. PF approximations of Fig. 5 in desirability space.

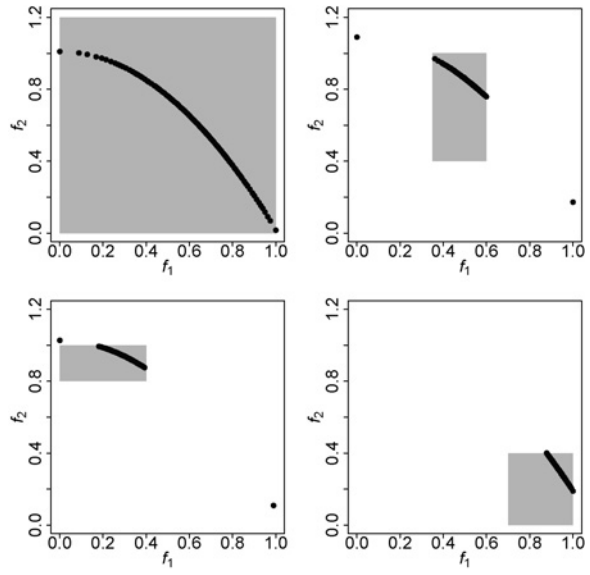

Fig. 7. Representative PF approximations of the DF-SMS-EMOA on ZDT2. The different target regions are highlighted by gray boxes which indicate the area of the objective space mapped to desirabilities $d_i \in [0.001, 0.999]$, $i = 1, 2$.

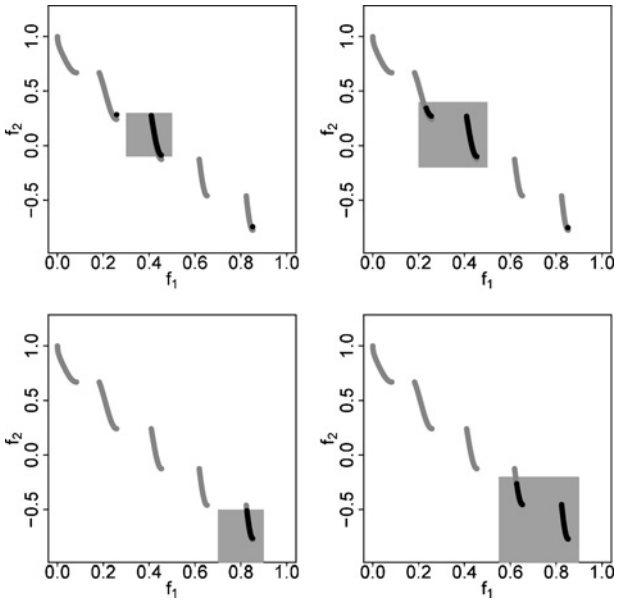

Fig. 8. Representative PF approximations of the DF-SMS-EMOA on ZDT3. The different target regions are highlighted by gray boxes which indicate the area of the objective space mapped to desirabilities $d_i \in [0.001, 0.999]$, $i = 1, 2$. The true PF of ZDT3 is shown in light gray.

that the SMS-EMOA part of the DF-SMS-EMOA is capable of approximating the hypervolume-optimal distribution. Only the positions of the extreme solutions do not agree with the optimal positions in the theoretical framework of Auger *et al.* [47]. Despite the choice of the closest possible reference point $\boldsymbol{R} = \mathbf{0}$, the extremes of the front in desirability space are often attained. Since Harrington's one-sided DF does not change the ordering of solutions, this leads to single solutions at the extremes of the true PF. Nevertheless, the bias toward the target region is so strong that a complete restriction to this region is almost successful. The occurrence of the extreme solutions of the true PF should not be seen as a drawback of the proposed procedure, but rather as a meaningful enhancement in order to give the DM an idea of the spread of all nondominated solutions.

In the cases where the thresholds of the desirabilities include the whole range of the PF, the DF-SMS-EMOA obtains an approximation set, which is widely spread (upper left plots of Figs. 5 and 7) over the whole PF. However, as shown in Fig. 9 for ZDT1 and ZDT2 based on histograms of the DI D_{GM} (3), the solutions are biased toward the knee points of the PF by means of the DF transformation in the DF-SMS-EMOA. In contrast to the SMS-EMOA, the density of solutions monotonically increases for higher D_{GM}. This result

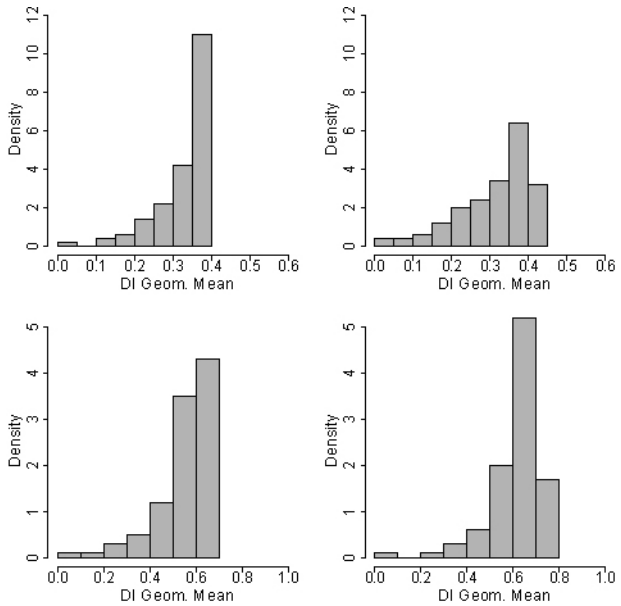

Fig. 9. Histograms of the D_{GM} values of the solutions in the PF approximation of ZDT1 (top, compare upper left plot of Fig. 5) and ZDT2 (bottom, compare upper left plot of Fig. 7). The histograms of the DF-SMS-EMOA are shown on the left-hand side. For comparison, the histograms of an approximation obtained by the standard SMS-EMOA are also provided (right).

confirms the assumptions theoretically motivated for linear PFs in Section IV also for convex and concave PFs. In relation to other preference articulation techniques in MOO, a distribution biased toward the desired part of the PF directly results from the objective transformation. The introduction of another parameter by using ε-dominance, often needed by reference point methods to provide a well-distributed approximation set around the reference point, is not necessary.

In real-world problems the location of the true PF is often only roughly known. Thus, situations can occur where the desired region does not cover the true PF. This problem was addressed by experiments in which this region is completely situated in the nondominated or in the dominated side of the front. By means of these experiments, an analysis on the sensitivity of the DF-SMS-EMOA with respect to target regions on and far from the true PF can be performed.

The results of the experiments are shown in Figs. 10, 11, and 13. The corresponding mapping of the objective values for the not appropriately specified target regions in desirability space is shown in Fig. 12 for ZDT2. The specification leads to transformed fronts with extreme convex and concave shapes for completely dominated and completely nondominated target regions, respectively. Notwithstanding, the SMS-EMOA part of the DF-SMS-EMOA is still able to provide an approximation that is close to the theoretically optimal distribution, i.e., the small region with an gradient $f_2'(f_1)$ close to one is densely covered while the ends of the PF with gradients $f_2'(f_1)$ close to zero or $-\infty$ are covered with single solutions only [47]. Consequently, the approximation set is restricted to objective values mapped to desirabilities $d > 0.001$ in case of dominated target regions. Furthermore, DF-SMS-EMOA can still provide solutions on the true PF due to the monotonicity of Harrington's one-sided DF. For the other

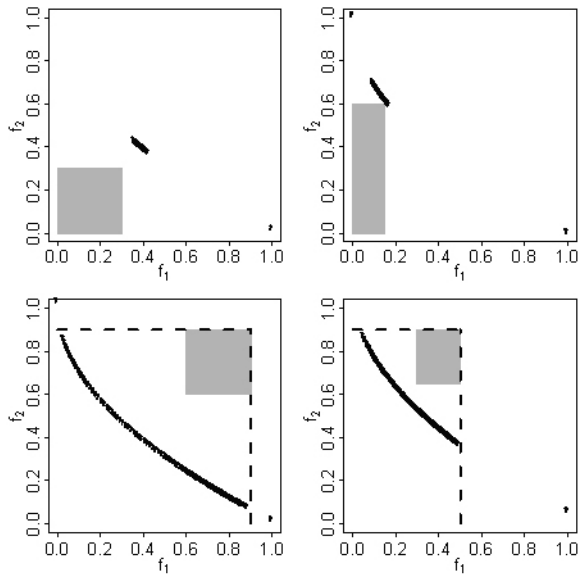

Fig. 10. Representative PF approximations of the DF-SMS-EMOA on ZDT1 for target regions not including the PF. The target regions are highlighted by gray boxes which indicate the area of the objective space mapped to desirabilities $d_i \in [0.001, 0.999]$, $i = 1, 2$.

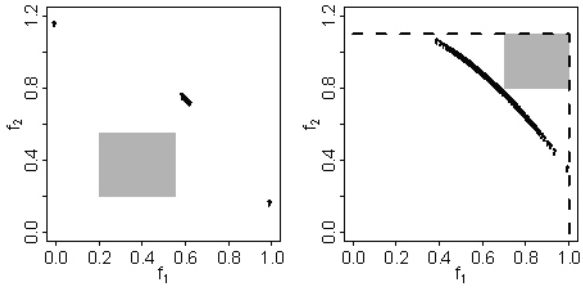

Fig. 11. Representative PF approximations of the DF-SMS-EMOA on ZDT2 for target regions not including the PF. The target regions are highlighted by gray boxes which indicate the area of the objective space mapped to desirabilities $d_i \in [0.001, 0.999]$, $i = 1, 2$.

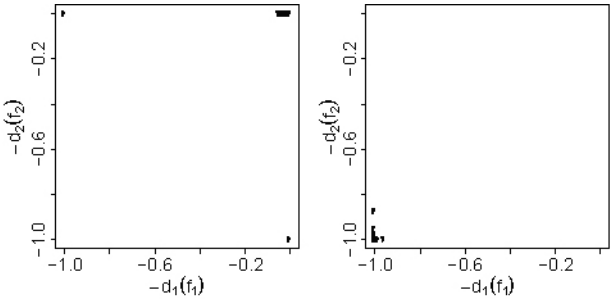

Fig. 12. PF approximations of Fig. 11 in desirability space.

case of completely nondominated target regions, the solutions cluster around the point of the true PF that is closest to the target region. Thus, the spread of the approximation is usually small. The internal adaptation of the DF (lines 7–10 of the pseudocode in Fig. 3) maintains the selection pressure toward the theoretically unattainable target region. As a result, the approximation quality of the SMS-EMOA in combination with the monotonicity of Harrington's one-sided DF and the internal

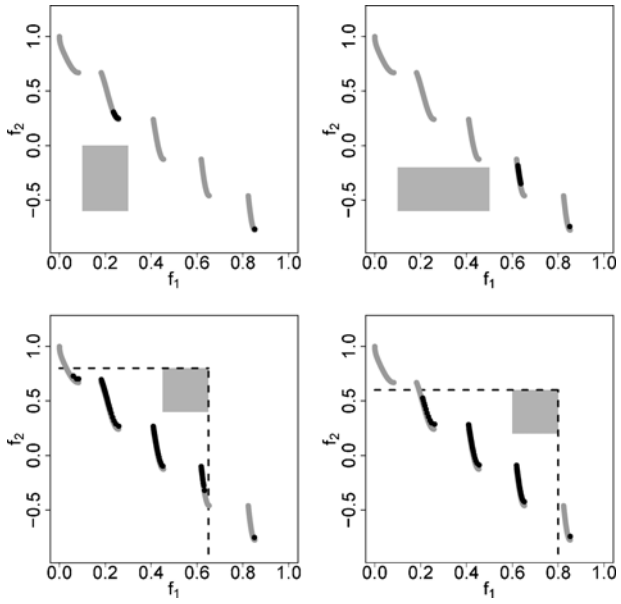

Fig. 13. Representative PF approximations of the DF-SMS-EMOA on ZDT3 for target regions not including the PF. The target regions are highlighted by gray boxes which indicate the area of the objective space mapped to desirabilities $d_i \in [0.001, 0.999]$, $i = 1, 2$. The true PF of ZDT3 is shown in light gray.

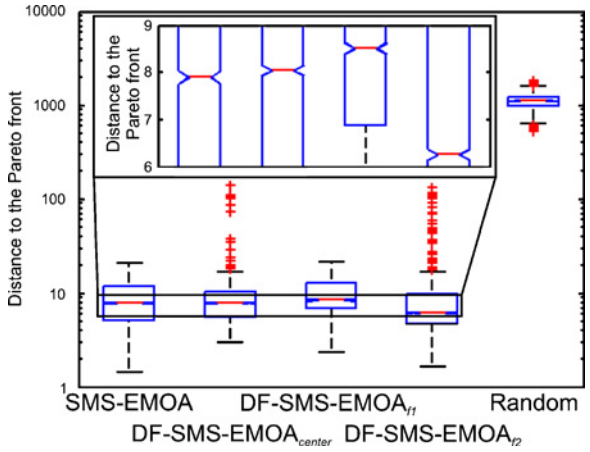

Fig. 14. Box plots of the distribution of the distances of the solutions in the PF approximations of the algorithm to the true PF. The distributions for the SMS-EMOA (on the left) and three variants of DF-SMS-EMOA focusing on different regions of the PF are shown. Each box has lines at the lower quartile, median, and upper quartile values. The whiskers show the extent of the rest of the data. The crosses represent outliers, i.e., data with values beyond the ends of the whiskers, which maximally extend to 1.5 units of the interquartile length. The notches represent a robust estimate of the uncertainty about the medians for box-to-box comparison. Boxes whose notches do not overlap indicate that the medians of the two groups differ at the 5% significance level.

adaptation of the DF limits makes DF-SMS-EMOA robust against not appropriately specified target regions.

B. Influence on Global Search Behavior

As a result of the previous experiments, the integration of preferences into the optimization often restricts the search of the EMOA to some preferred objective regions. Thus, the effect of the preference integration on the global search behavior was analyzed by using the standard SMS-EMOA and three variants of the DF-SMS-EMOA with different target regions. For all DF-SMS-EMOA variants and all objectives, the first tuple was set to $(Y^{(1)}, d^{(1)}) = (0, 0.99)$. The first variant DF-SMS-EMOA$_{\text{center}}$ is parameterized with $(Y^{(2)}, d^{(2)}) = (0.5, 0.01)$ for both objective functions in order to strongly focus on the knee in the center of the PF. The second variant DF-SMS-EMOA$_{f1}$ uses a DF with $(Y_1^{(2)}, d_1^{(2)}) = (0.1, 0.01)$ and $(Y_2^{(2)}, d_2^{(2)}) = (100, 0.01)$. Thus, only very low values of the first objective f_1 are desirable. The last variant DF-SMS-EMOA$_{f2}$ focuses on low values of the second objective f_2 by using the DF parameterizations $(Y_1^{(2)}, d_1^{(2)}) = (1, 0.9)$ and $(Y_2^{(2)}, d_2^{(2)}) = (0.1, 0.01)$.

The comparison between the variants is performed by means of boxplots of the distributions of the results. In order to create the box of an EMOA, the distance to the true PF was computed for each solution in the 50 final approximation sets. We are focusing only on the distance to the PF since the distribution of the solutions is biased by the preferences (compare Section V-A). Thus, no fair criterion for a comparison can be formulated. Since the population size was set to $\mu = 100$, each box is calculated based on 5000 distance values. The computation of a mean or median for each run was avoided to not lose information about the distribution of the distance values.

The results of the experiment are shown in Fig. 14. All EMOAs find much better results than a random sample of 100 solutions in the search space. From a global view (lower plot), no significant differences between the algorithms can be observed. The outliers (crosses) for variants focusing on center of the PF and on the second objective are due to the solutions covering the optimal value for the first objective. Since the transformed values of the second objective are close to zero for all solutions in the vicinity of this extremum, no pressure toward an improvement in the second objective can be maintained.

A closer analysis of the robust median estimates over all runs (zoom box in Fig. 14) shows that there are indeed significant differences between the algorithms. These differences are not caused by the focus on a certain region, but by the focus on a specific objective. While DF-SMS-EMOA$_{f1}$ focusing on the first objective of ZDT1 results in a worse median distance compared to SMS-EMOA ($p \ll 0.01$ in a nonparametric Kruskal–Wallis test), the focus of DF-SMS-EMOA$_{f2}$ on the second objective can actually improve the median distance ($p \ll 0.01$). Between the SMS-EMOA and DF-SMS-EMOA$_{\text{center}}$, no significant differences between the median estimates can be detected. In conclusion, the experiments show that the integration of preferences does not necessarily deteriorate the global search performance. In particular, a focus on the objective that is harder to optimize can improve the results of the EMOA since the resources are concentrated on this objective.

C. Application to the Optimization of a Turning Process

The turning optimization problem that is considered as application in this paper has been introduced by Biermann *et al.* [50]. It broaches the issue of parameterizing turning

processes for graded materials with properties which change over the dimensions of the workpiece from ductile to hard and vice versa. These turning processes are challenging since recommendations are only available for one of these cases, and not all parameters can be changed during the process [50]. The cutting parameters for which suitable parameters have to be found are cutting speed $v_c \in$ [50 m/min, 100 m/min], feed $f \in$ [0.1 mm, 0.25 mm], and cutting depth $a_p \in$ [0.1 mm, 0.25 mm], where the domain of the parameters is based on recommendations of the tool manufacturer.

The objectives of the turning problem are the following:

1) Y_1, the primary processing time t_p (min);
2) Y_2, the roughness in the ductile region of the workpiece Rz_{duct} (μm);
3) Y_3, the roughness in the hard region of the workpiece Rz_{hard} (μm);
4) Y_4, the width of flank wear land on the major cutting edge $VB_{\text{max,major}}$ (μm);
5) Y_5, the width of flank wear land on the minor cutting edge $VB_{\text{max,minor}}$ (μm).

The first objective is directly related to the efficiency of the process. As faster the process can be realized, as more turning operations can be performed. The objectives Y_2–Y_5 are established statistics to evaluate the quality of the surface and the wear of the cutting tool. Their calculation is described in Fig. 15. Despite the existence of two pairs of objectives describing equal properties in different regions, no objectives can be reduced without allowing major changes in equivalence classes of the dominance relation [50]. In order to render the application of metaheuristics possible, the five objectives were represented by nonlinear statistical surrogate models, which were calculated based on experimental measurements [50].

For all objectives, preferences with respect to specific intervals exist. While t_p, $VB_{\text{max,major}}$, and $VB_{\text{max,minor}}$ should be strictly minimized, roughnesses lower than 2 μm do not provide any improvement. Furthermore, critical values that must not be exceeded exist for all objectives by means of engineer standards. For the width of flank wear land, a value above 300 μm has to be classified as tool failure. Roughnesses higher than 3 μm violate demands on fine machining. Thus, the DFs for the objective transformation were parameterized with

$$\begin{aligned}
(Y_1^{(1)}, d_1^{(1)}) &= (0, 0.99) \quad (Y_1^{(2)}, d_1^{(2)}) = (30, 0.01)\\
(Y_2^{(1)}, d_2^{(1)}) &= (2, 0.99) \quad (Y_2^{(2)}, d_2^{(2)}) = (3, 0.01)\\
(Y_3^{(1)}, d_3^{(1)}) &= (2, 0.99) \quad (Y_3^{(2)}, d_3^{(2)}) = (3, 0.01)\\
(Y_4^{(1)}, d_4^{(1)}) &= (0, 0.99) \quad (Y_4^{(2)}, d_4^{(2)}) = (300, 0.01) \text{ and}\\
(Y_5^{(1)}, d_5^{(1)}) &= (0, 0.99) \quad (Y_5^{(2)}, d_5^{(2)}) = (300, 0.01).
\end{aligned}$$

The combination of the objectives of the turning problem and DFs to describe the preferences of the DM has not been performed before. Thus, single-objective maximizations of the two DIs D_{GM} and D_{MM} were performed beforehand using the MATLAB implementation[2] of Hansen's covariance matrix adaption evolution strategy (CMA-ES) [51] in order to find a suitable compromise as a reference solution and to evaluate the hardness of the transformed problem. The CMA-ES was chosen because it has proven its applicability to real-world problems many times. The tolerances for decision and objective space are set to $\varepsilon = 1.1 \times 10^{-16}$ and box constraints are defined in order to find parameter values in the before mentioned intervals. All other parameters are used with their default values. For D_{GM} only half of the 10 runs provided an acceptable value of $D_{\text{GM}} = 0.3071$ for the parameter vector $v_c = 73.7$ m/min, $f = 0.105$ mm, and $a_p = 0.250$ mm. The other half is stopped directly based on the stopping criterion of equal function evaluations for all solutions, which is caused by DF values below the machine accuracy. For D_{MM}, the number of prematurely terminated runs based on the equal-functions-evaluations criterion increases to 7 of 10. The optimal value, found in only 2 of the runs, is $D_{\text{MM}} = 0.1336$ ($v_c = 73.8$ m/min, $f = 0.120$ mm, and $a_p = 0.250$ mm). In one of the runs, a local optimum of $D_{\text{MM}} = 0.0273$ ($v_c = 78.7$ m/min, $f = 0.100$ mm, and $a_p = 0.250$ mm) was found. These results indicate that the areas of interest are very small and surrounded by a plateau of desirabilities below the machine accuracy ε.

The approximations of the PF of the turning problem obtained by DF-SMS-EMOA and SMS-EMOA without preference information are shown in Fig. 16. In each projection of the matrix, the lower left box of the dotted grid contains the solutions of interest, which is depicted by gray boxes in the plots. The application of the DF-SMS-EMOA was successful since a big cluster of points is situated in this target region for each projection. Furthermore, the histograms in the diagonal document that the vast majority of solutions of DF-SMS-EMOA can meet the specified preferences for three of the five objectives. Only for the objectives related to roughnesses, a second mode with infeasible values exists. In contrast, the standard SMS-EMOA is not able to find solutions that satisfy the specifications for the primary processing time t_p. This is mainly due to a strong focus on the objectives Y_4 and Y_5 related to wear. These objectives are all within the lower tenth of their objective range. This result confirms the statement of Branke and Deb [6] that different objective scales lead to biased distributions of the solutions on the PF. In this case, the domain of the wear criteria is ten times as big as the domain of the primary production time and hundred times as big as the domain of the roughness criteria. On the contrary, the transformation of the objectives by means of DFs allows a fair tradeoff of the objectives to be computed.

For the DF-SMS-EMOA, a quarter of the 100 solutions in the PF approximation obtains a DI of $D_{\text{GM}} > 0.01$. Consequently, no restarts of the algorithm have to be performed in order to find a suitable solution. Moreover, every tenth solution obtains a DI of $D_{\text{GM}} > 0.2$. Thus, a set of desirable alternatives can be presented to the DM. The results of Section V-A with respect to the focus on a given region and the high density around good compromise solutions can be confirmed on the practical problem. Even for the minimum desirability D_{MM}, which is not directly related to the hypervolume indicator, still more than a tenth of the 100 solutions obtain $D_{\text{MM}} > 0.01$. For these solutions, the minimum requirements of each objective are achieved. For both indicators, a solution with the optimal

[2]http://www.lri.fr/~hansen/cmaes_inmatlab.html.

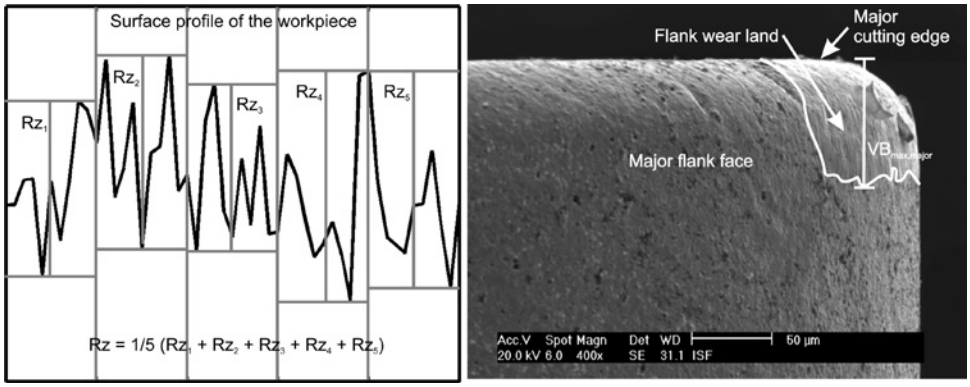

Fig. 15. Graphical explanation of the objectives related to the quality of the turned surface (Rz, left) and the wear of the cutting tool ($VB_{\max,\text{major}}$, right). For the calculation of the surface roughness, the scanned surface profile is divided in five uniform parts. In each part, the distance between the minimum and maximum profile height is determined. The indicator of the surface roughness Rz is the mean of the five computed distances. $VB_{\max,\text{minor}}$ can be determined analogously to $VB_{\max,\text{major}}$ (right) based on a scanning electro micrograph of the minor flank face.

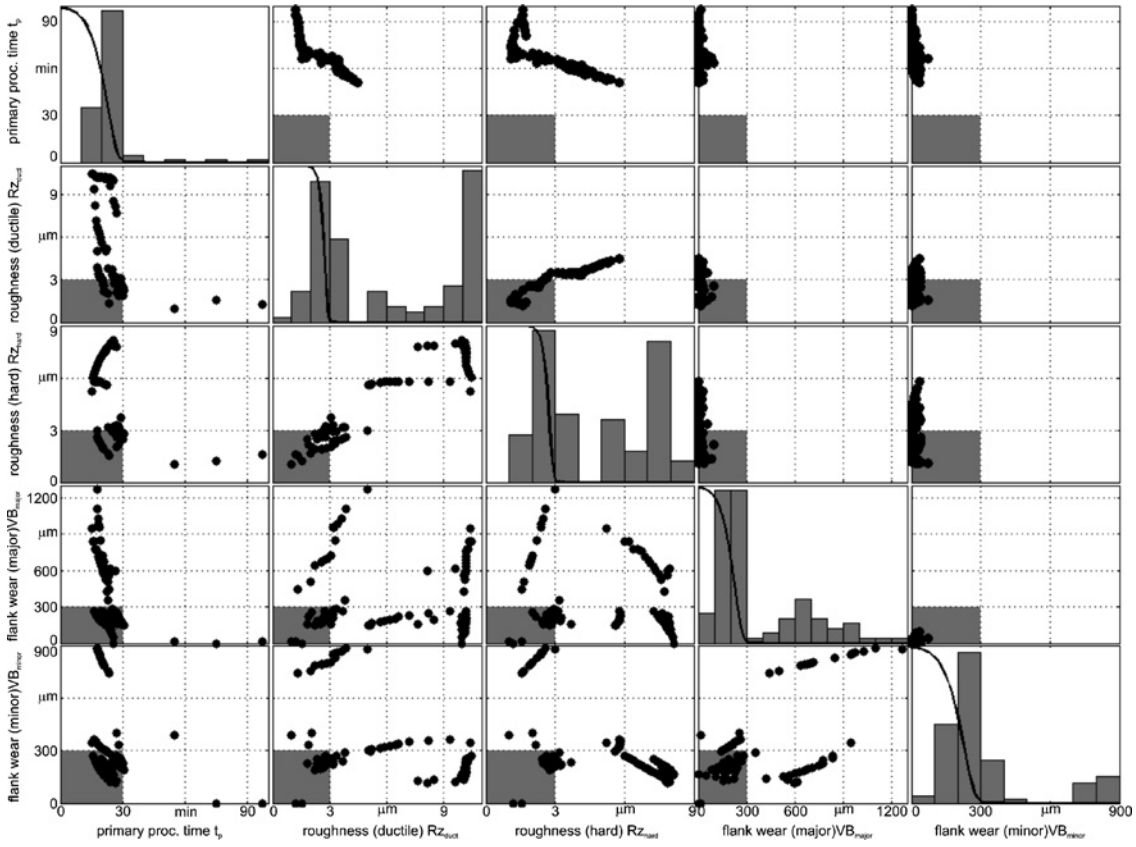

Fig. 16. Scatter matrix of the PF approximations found by DF-SMS-EMOA (lower left) and SMS-EMOA without preference information (upper right). In the diagonal, the DFs and histograms for each objective used by DF-SMS-EMOA are provided in order to analyze the distribution of values with respect to the specified preferences. Moreover, the target regions are highlighted by gray boxes which indicate the area of the objective space projection mapped to desirabilities $d_i \in [0.01, 0.99]$, $i = 1, \ldots, 5$.

parameter vector found by the CMA-ES is part of the PF approximation.

Regarding the premature termination of the CMA-ES based on equal function evaluations due to the machine accuracy, the proposed online-adjustment of the DFs during the optimization was an important factor for the successful application of the DF-SMS-EMOA. Even after 20 000 FE, the bounds on the roughnesses are still adjusted to $(Y_2^{(2)}, d_2^{(2)}) = (5.02, \varepsilon)$ and $(Y_3^{(2)}, d_3^{(2)}) = (3.70, \varepsilon)$, which assists in guiding the algorithm to the desired area. The insistence of this adjustment can be explained by the second mode of high roughnesses in the histograms of Fig. 16. For these roughnesses, desirabilities below the machine accuracy ε are assigned, leading to an adjustment of the corresponding DFs. For an increasing objective dimension d, also the dimension of subspaces of the PF with extremal values in one of the objectives increases to $d-1$. Since the hypervolume indicator performs a kind of geometrical aggregation, which does not penalize low values in a single objective as strong as the minimum approach, the median of the objective values cannot be improved toward the given specification limits.

However, the number of solutions in the desired objective region is still high enough to allow the DM a decision based on a set of good compromise solutions and to obtain an understanding of the Pareto set. For all solutions in the sets of feasible solutions (D_{GM} and $D_{\mathrm{MM}} > 0.01$, respectively), the cutting depth a_p is set to the maximum value of $a_p = 0.25$ mm. Thus, an increase of the cutting depth beyond the recommendations of the tool manufacturer seems promising. For the feed f, values between $f = 0.1$ mm and $f = 0.12$ mm result, where, interestingly, the lower value is optimal based on D_{GM} and the upper value is optimal based on D_{MM}. A lower feed f reduces the roughness and the wear, but results in higher primary processing times t_p [52]. Thus, the availability of further compromise solutions between these extremes assists the DM in finding an appropriate parameter vector. The range of the cutting speed in this sets is $v_c \in [66.2$ m/min, 81.4 m/min]. Therefore, the objectives are not as sensitive with respect to the cutting speed v_c. Nevertheless, the optimal value of v_c is very close for both desirability indices.

The difference between the optimal results for the different desirability indices with respect to the feed f is based on the primary processing time t_p being the critical objective due to the strong negative correlation to the other objectives. In combination with the bias introduced by the objective scaling, this negative correlation leads to the absence of solutions meeting the preferences for the primary processing time t_p in the approximation of SMS-EMOA. In contrast, the dynamic tradeoff between the solution during the optimization, which is induced by the nonlinear DFs, allows DF-SMS-EMOA to focus on the primary processing time t_p as long as no feasible values are found for this objective. Thus, despite the objective-wise definition of the DFs, correlations between the objectives can be considered.

In conclusion, the use of the DF-SMS-EMOA allows the integration of preferences in the considered practical optimization problem. Compared to a single-objective optimization of the different desirability indices and the MOO without preference information, DF-SMS-EMOA robustly provides a set of solutions that is restricted to the preferences of the DM. Furthermore, the availability of many compromise solutions allows a better analysis of the solutions in decision space, which is of practical interest since the final parameters are to be identified there. In the example provided in this paper, a change of the feed f allows the objectives to be balanced against each other. Furthermore, an increase of the cutting depth a_p beyond the recommendations of the tool manufacturer may offer the potential of improving the primary production time t_p without significantly deteriorating the wear and roughness criteria.

VI. Conclusion

In this paper, an approach for integrating preferences into the $\mathcal{S}$-metric selection evolutionary multiobjective algorithm (SMS-EMOA) by transforming the objectives based on DFs has been presented. DFs represent an intuitive and flexible objective transformation, and, thus, allow a straightforward specification of the preferences of the DM. The resulting DF-SMS-EMOA accomplishes to restrict to specified target regions of the PF. In cases where the target region covers the true PF, DF-SMS-EMOA exclusively obtains solutions in this target region besides one or two extreme boundary solutions. The procedure also generates reasonable approximation sets when inappropriate target regions are specified. In case of unattainable target regions, the algorithm provides solutions as close to the desired region as possible. In case of dominated target regions, the DF-SMS-EMOA further converges to the true PF. Experiments on a multimodal test function have shown that the global search quality of EMOA was not seriously affected by the objective transformation. In contrast, a focus on the objective which is harder to optimize can improve the results.

Furthermore, the combination of $\mathcal{S}$-metric selection and DFs tackles the critical issue of different scales and units of the objectives, as well as the selection of the reference point for the hypervolume computation. Both aspects support the applicability to practical optimization problems. In this paper, an exemplary specification of DFs for a complex turning process has been provided. In this problem, as well as in related applications, the desired ranges are often motivated by engineer standards. In contrast to SMS-EMOA without preference information, DF-SMS-EMOA accomplishes to detect a set of solutions meeting all specified requirements. The distribution of the solutions was strongly biased toward the desired regions. In particular, the adaptive scaling of the upper desirability bounds has proven to support the applicability for problems on which only a very small area of the search space is feasible.

However, with an increasing number of objectives the number of border solutions outside the specification limits of single DFs also increases. The same holds for the complexity of the hypervolume computation. Consequently, further research will focus on combinations of EMOAs and DFs for many-objective problems. Furthermore, it will be investigated whether the results in noisy environments [17] can be transferred to the DF-

SMS-EMOA. A tool for the graphically assisted specification of the DFs is currently being implemented.

REFERENCES

[1] E. Zitzler and S. Künzli, "Indicator-based selection in multiobjective search," in *Proc. PPSN*, 2004, pp. 832–842.

[2] T. Wagner, N. Beume, and B. Naujoks, "Pareto-, aggregation-, and indicator-based methods in many-objective optimization," in *Proc. EMO*, 2007, pp. 742–756.

[3] E. Zitzler, L. Thiele, and J. Bader, "SPAM: Set preference algorithm for multiobjective optimization," in *Proc. PPSN*, 2008, pp. 847–858.

[4] E. Zitzler, L. Thiele, M. Laumanns, C. Fonseca, and V. Fonseca, "Performance assessment of multiobjective optimizers: An analysis and review," *IEEE Trans. Evol. Comput.*, vol. 8, no. 2, pp. 117–132, Apr. 2003.

[5] J. Harrington, "The desirability function," *Ind. Quality Contr.*, vol. 21, no. 10, pp. 494–498, 1965.

[6] J. Branke and K. Deb, "Integrating user preferences into evolutionary multiobjective optimization," in *Knowledge Incorporation in Evolutionary Computation*. Berlin/Heidelberg, Germany: Springer, 2004, pp. 461–478.

[7] M. Emmerich, N. Beume, and B. Naujoks, "An EMO algorithm using the hypervolume measure as selection criterion," in *Proc. 3rd Int. Conf. EMO*, 2005, pp. 62–76.

[8] N. Beume, B. Naujoks, and M. Emmerich, "SMS-EMOA: Multiobjective selection based on dominated hypervolume," *Eur. J. Oper. Res.*, vol. 181, no. 3, pp. 1653–1669, 2007.

[9] J. Branke, "Consideration of partial user preferences in evolutionary multiobjective optimization," in *Multiobjective Optimization*, vol. 5252. 2008, pp. 157–178.

[10] C. A. Coello Coello, "Handling preferences in evolutionary multiobjective optimization: A survey," in *Proc. IEEE CEC*, 2000, pp. 30–37.

[11] L. Rachmawati and D. Srinivasan, "Preference incorporation in multiobjective evolutionary algorithms: A survey," in *Proc. IEEE CEC*, 2006, pp. 962–968.

[12] A. Jaszkiewicz and J. Branke, "Interactive multiobjective evolutionary algorithms," in *Multiobjective Optimization*, vol. 5252. 2008, pp. 179–193.

[13] S. F. Adra, I. Griffin, and P. J. Fleming, "A comparative study of progressive preference articulation techniques for multiobjective optimization," in *Proc. EMO*, vol. 4403. 2006, pp. 908–921.

[14] C. Coello Coello, "Theoretical and numerical constraint-handling techniques used with evolutionary algorithms: A survey of the state-of-the-art," *Comput. Methods Appl. Mech. Eng.*, vol. 191, no. 11–12, pp. 1245–1287, Jan. 2002.

[15] J. Branke, K. Deb, H. Dierolf, and M. Osswald, "Finding knees in multiobjective optimization," in *Proc. PPSN*, vol. 3242. 2004, pp. 722–731.

[16] J. Mehnen, H. Trautmann, and A. Tiwari, "Introducing user preference using desirability functions in multiobjective evolutionary optimization of noisy processes," in *Proc. IEEE CEC*, 2007, pp. 2687–2694.

[17] H. Trautmann and J. Mehnen, "Preference-based Pareto-optimization in certain and noisy environments," *Eng. Optmiz.*, vol. 41, no. 1, pp. 23–38, Jan. 2009.

[18] K. Deb, A. Pratap, and S. Agarwal, "A fast and elitist multiobjective genetic algorithm: NSGA-II," *IEEE Trans. Evol. Comput.*, vol. 6, no. 8, pp. 182–197, Apr. 2002.

[19] A. Messac, "Physical programming: Effective optimization for computational design," *AIAA J.*, vol. 34, no. 1, pp. 149–158, 1996.

[20] S. Utyuzhnikov, P. Fantini, and M. Guenov, "Numerical method for generating the entire Pareto frontier in multiobjective optimization," in *Evolutionary and Deterministic Methods for Design, Optimization and Control with Applications to Industrial and Societal Problems*. Munich, Germany: EUROGEN, 2005.

[21] J. Branke, T. Kaußler, and H. Schmeck, "Guidance in evolutionary multiobjective optimization," *Adv. Eng. Soft.*, vol. 32, no. 6, pp. 499–507, Jun. 2001.

[22] C. M. Fonseca and P. J. Fleming, "Genetic algorithms for multiobjective optimization: Formulation, discussion and generalization," in *Proc. 5th Int. Conf. Genet. Algorithms*, 1993, pp. 416–423.

[23] K. Deb and J. Sundar, "Reference point based multiobjective optimization using evolutionary algorithms." in *Proc. GECCO*, 2006, pp. 635–642.

[24] K. Deb and A. Kumar, "Light beam search based multiobjective optimization using evolutionary algorithms," in *Proc. IEEE Congr. Evol. Comput.*, 2007, pp. 2125–2132.

[25] G. W. Greenwood, X. Hu, and J. G. D'Ambrosio, "Fitness functions for multiple objective optimization problems: Combining preferences with Pareto rankings," in *Proc. FOGA*, 1996, pp. 437–455.

[26] E. Zitzler, D. Brockhoff, and L. Thiele, "The hypervolume indicator revisited: On the design of Pareto-compliant indicators via weighted integration," in *Proc. Conf. EMO*, vol. 4403. 2007, pp. 862–876.

[27] J. Wang, J. Zhang, and X. Wei, "Evolutionary multiobjective optimization algorithm with preference for mechanical design," in *Proc. ICMLC*. vol. 3930. 2005, pp. 497–506.

[28] S. Greco, B. Matarazzo, and R. Slowinski, "Dominance-based rough set approach to interactive multiobjective optimization," in *Multiobjective Optimization*, vol. 5252. Berlin, Germany: Springer, 2008, pp. 121–155.

[29] J. R. Figueira, S. Greco, V. Mousseau, and R. Slowinski, "Interactive multiobjective optimization using a set of additive value functions," in *Multiobjective Optimization*, vol. 5252. Berlin, Germany: Springer, 2008, pp. 97–119.

[30] K. Deb and A. Kumar, "Interactive evolutionary multiobjective optimization and decision-making using reference direction method," in *Proc. 9th Ann. GECCO*, 2007, pp. 781–788.

[31] J. Branke, S. Greco, R. Slowinski, and P. Zielniewicz, "Interactive evolutionary multiobjective optimization using robust ordinal regression," in *Proc. EMO*, vol. 5467. 2009, pp. 554–568.

[32] I. C. Parmee and D. Cvetkovic, "Preferences and their application in evolutionary multiobjective optimization," *IEEE Trans. Evol. Comput.*, vol. 6, no. 1, pp. 42–57, Feb. 2002.

[33] M. Köksalan and S. Phelps, "An evolutionary metaheuristic for approximating preference-nondominated solutions," *Inform. J. Comput.*, vol. 19, no. 2, pp. 291–301, 2007.

[34] S. P. Phelps and M. Köksalan, "An interactive evolutionary metaheuristic for multiobjective combinatorial optimization," *Manage. Sci.*, vol. 49, no. 12, pp. 1726–1738, 2003.

[35] A. Sülflow, N. Drechsler, and R. Drechsler, "Robust multiobjective optimization in high dimensional spaces," in *Proc. EMO*, vol. 4403. 2006, pp. 715–726.

[36] U. K. Wickramasinghe and X. Li, "Integrating user preferences with particle swarms for multiobjective optimization," in *Proc. 10th Ann. Conf. GECCO*, 2008, pp. 745–752.

[37] H. Ishibuchi, Y. Nojima, K. Narukawa, and T. Doi, "Incorporation of decision maker's preference into evolutionary multiobjective optimization algorithms," in *Proc. 8th Ann. Conf. GECCO*, 2006, pp. 741–742.

[38] F. di Pierro, S. T. Khu, and D. A. Savic, "An investigation on preference order ranking scheme for multiobjective evolutionary optimization," *IEEE Trans. Evol. Comput.*, vol. 11, no. 1, pp. 17–45, Feb. 2007.

[39] E. Fernandez and R. Olmedo, "An improved method for deriving final ranking from a fuzzy preference relation via multiobjective optimization," *Found. Comput. Decision Sci.*, vol. 28, no. 3, pp. 143–157, 2003.

[40] E. Fernandez and J. C. Leyva, "A method based on multiobjective optimization for deriving a ranking from a fuzzy preference relation," *Eur. J. Oper. Res.*, vol. 154, no. 1, pp. 110–124, Apr. 2004

[41] Y. Jin and B. Sendhoff, "Incorporation of fuzzy preferences into evolutionary multiobjective optimization," in *Proc. GECCO*, 2002, p. 683.

[42] H. Trautmann and C. Weihs, "On the distribution of the desirability index using Harrington's desirability function," *Metrika*, vol. 63, no. 2, pp. 207–213, 2006.

[43] T. Wheldon, *Mathematical Models in Cancer Research*. Bristol, PA: Adam Hilger, 1988.

[44] K.-J. Lin and D. Lin, "Simultaneous optimization of mechanical properties of steel by maximizing desirability functions," *Appl. Stat.*, vol. 49, no. 3, pp. 311–326, 2000.

[45] K. Deb, *Multiobjective Optimization Using Evolutionary Algorithms*. Chichester, U.K.: Wiley, 2001.

[46] D. E. Goldberg, *Genetic Algorithms in Search, Optimization, and Machine Learning*. Reading, MA: Addison-Wesley, 1989.

[47] A. Auger, J. Bader, D. Brockhoff, and E. Zitzler, "Theory of the hypervolume indicator: Optimal μ-distributions and the choice of the reference point," in *Proc. FOGA*, 2009, pp. 87–102.

[48] N. Beume, C. M. Fonseca, M. López-Ibáñez, L. Paquete, and J. Vahrenhold, "On the complexity of computing the hypervolume indicator," *IEEE Trans. Evol. Comput.*, vol. 15, no. 5, pp. 1075–1082, Oct. 2009.

[49] E. Zitzler, K. Deb, and L. Thiele, "Comparison of multiobjective evolutionary algorithms: Empirical results," *Evol. Comput.*, vol. 8, no. 2, pp. 173–195, 2000.

[50] D. Biermann, K. Weinert, and T. Wagner, "Model-based optimization revisited: Toward real-world processes," in *Proc. IEEE CEC*, Jun. 2008, pp. 2980–2987.

[51] N. Hansen and A. Ostermeier, "Completely derandomized self-adaptation in evolution strategies," *Evol. Comput.*, vol. 9, no. 2, pp. 159–195, 2001.
[52] D. Biermann, A. Zabel, S. Grünert, and B. Sieben, "Machining of functional graded workpieces," in *Proc. 3rd CIRP Int. Conf. HPC*, 2008, pp. 723–732.
[53] S. Obayashi, K. Deb, C. Poloni, T. Hiroyasu, and T. Murata, Eds., "Evolutionary multicriterion optimization," in *Proc. 4th Int. Conf. EMO*, vol. 4403. 2007.
[54] J. Branke, K. Deb, K. Miettinen, and R. Slowinski, Eds., *Multiobjective Optimization, Interactive and Evolutionary Approaches (Outcome of Dagstuhl Seminars)*, vol. 5252. Berlin, Germany: Springer, 2008.

Tobias Wagner studied computer science at the Technische Universität Dortmund, Dortmund, Germany.

Since 2006, he has been with the Institute of Machining Technology, Technische Universität Dortmund (Institut für Spanende Fertigung). His current research interests include enhancements of statistical modeling techniques for providing surrogates for objectives of production-engineering problems and the application of these models within single and multiobjective optimization algorithms.

Heike Trautmann studied statistics at the Technische Universität Dortmund, Dortmund, Germany. She received the Ph.D. degree from the Graduate School of Production Engineering and Logistics, Technische Universität Dortmund, in 2004.

She worked with a consulting company for 2 years. She is currently with the Department of Computational Statistics, Technische Universität Dortmund. Her current post-doctoral research interests at the Department of Computational Statistics include multicriteria optimization, evolutionary algorithms, desirability indices, and statistical process control.